Experimental assessment of the lumped lithium-ion battery model

Tanılay Özdemir[1,*], *Ali* Amini[1], *Özgür* Ekici[1] and *Murat* Köksal[1]

[1]Department of Mechanical Engineering, Hacettepe University, 06800, Beytepe, Ankara, Turkey

Abstract. In this study, an axisymmetric computational lumped model is used to investigate the thermal and electrical behavior of a cylindrical Lithium-ion (Li-ion) battery during various discharging processes at 0-20-50°C operating temperatures. A typical cylindrical Li-ion cell consists of multiple spiral layers, on the other hand, the model employs the lumped battery interface approach in COMSOL Multiphysics to reduce the computational effort. In the lumped approach, layers of different materials are approximated as a uniform material with effective properties. Among other parameters, the Open Circuit Voltage (OCV) as a function of the State of Charge (SOC) is determined experimentally and used as input to the model. The model is then used to analyze the effects of the correlations of various parameters on the transient electrical and thermal responses of the battery and validated by comparing predicted results with experimental data.

1 Introduction

The first commercial Li-ion battery was introduced by Sony in 1991[1]. Nowadays Li-ion batteries can be found in almost every application to store the required electrical energy. They have been widely used due to their prominent advantages such as high specific energy and power, long cycling life, and relatively low self-discharge rate. However, their construction causes heat production from the battery during charging and discharging processes [2]. The heat generation within the cell is investigated by Bernardi et al. and defined in a simplified form as reversible and irreversible heat generation [3].

Among the two heat generation terms, there are some cases that neglect the effects of the reversible heat generation on cells thermal behavior [4,5]. However, it considerably impacts cell thermal behavior during the charging or discharging processes below the 1C rate currents. Therefore, in some researches, the entropic term is considered either as constant [6,7], or variable as a function of the SOC [8,9].

The generated heat cannot be completely dissipated by convection and radiation from the cell during charging and discharging processes. It also accumulates within the cell so that an increment in the temperature of the cell is inevitable. This shows that the thermal behavior of the battery should be examined thoroughly to provide a safe operating condition.

In this study, an axisymmetric computational model of a cylindrical Li-Ion battery is developed to investigate the thermal and electrical behavior of the battery during 0.5-1-1.5C discharging processes at 0-20-50°C ambient temperatures. In the experimental part, a battery testing system is used to determine the quality and performance of Li-ion batteries by applying simulated loads under computer control. At last, the experimental and simulation results are compared and found to be in a good agreement.

2 Anaylsis and modeling

In the lumped approach, layers of different materials are approximated as a uniform material with effective properties. Table 1 shows the parameters that were utilized in the lumped model interface.

Table 1. The lumped model parameters.

Description	Expression
Thickness of battery canister	4E-4 m
Battery radius	0.009 m
Battery height	0.065 m
Battery thermal conductivity, angular	28.05 W/(m·K)
Battery thermal conductivity, radial	3 W/(m·K)
Battery density	2782 kg/m³
Battery heat capacity	750 J/(kg·K)
Nominal Capacity of the Cell	3.25 Ah
Dimensionless charge exchange current	0.8
Diffusion time constant	1000 s
Initial state-of-charge	1
Heat capacity of the canister at constant pressure	875 J/(kgK)
Density of the canister	2059 kg/m³
Thermal conductivity of the canister	0.638W/(mK)

The model is then used to predict the instantaneous voltage values of the cell during various discharging

* Corresponding author: tanilayozdemir@hacettepe.edu.tr

processes at different ambient conditions. Thus, the generated heat within the cell is determined and the energy conservation equation is used in order to predict the temperature variation of the cell with respect to time. The model also predicts the state of charge (SOC) value of the cell using Eq. (1) [10].

$$\frac{\partial SOC}{\partial t} = \frac{I_{cell}}{Q_{cell,0}} \quad (1)$$

2.1. Voltage prediction

The lumped model uses the overpotential terms and the OCV values in order to estimate the voltage variation of the cell during discharging processes. The battery cell voltage is defined in Eq. (2) [10].

$$V_{cell} = OCV(SOC,T) + \eta_{ohmic} + \eta_{concentration} + \eta_{activation} \quad (2)$$

where, OCV represents the open circuit voltage of the cell and depends on the state of charge (SOC) and the temperature values of the cell. OCV values were determined with an experiment for various DOD (Depth of Discharge) values and the following curve was obtained from the 1C discharging process at 20°C reference temperature.

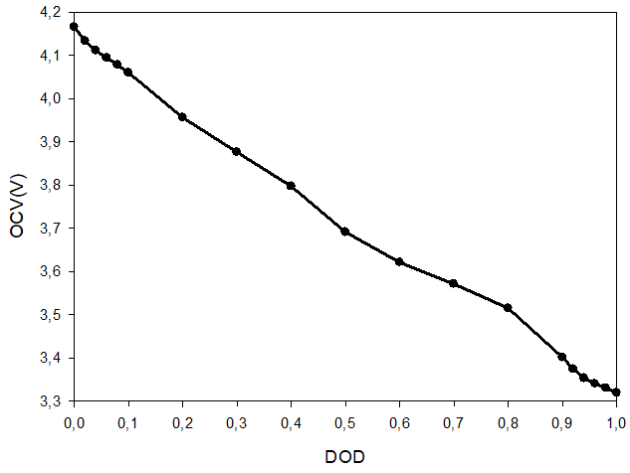

Fig. 1. Variation of OCV with DOD.

In the lumped model, the cell overpotential determines the voltage losses within the cell due to three main aspects. These terms are represented as ohmic, activation, and concentration overpotentials. The ohmic overpotential defines the voltage loss associated with the ohmic process in the electrolyte and electrodes. It is mainly caused by ionic resistance in the electrolyte. The lumped ohmic overpotential is determined as,

$$\eta_{ohmic} = \eta_{ohmic,1C} \frac{I_{cell}}{I_{1C}} \quad (3)$$

where $\eta_{ohmic,1C}$ represents the ohmic overpotential during 1C rate discharging process [10]. The cell discharge current at 1C is 3.25 Amp since the nominal capacity of the Li-ion cell is 3.25 Ah.

Activation overpotential is related to the charge transfer processes in the battery. The activation overpotential in the lumped model is calculated from the Eq. (4) [10]

$$\eta_{activation} = \frac{2RT}{F} \operatorname{asinh}\left(\frac{I_{cell}}{2J_0 I_{1C}}\right) \quad (4)$$

In this lumped model, concentration overpotential effects were modeled based on diffusion in an idealized particle. The lumped voltage loss associated with concentration overpotential is defined in Eq. (5) [10].

$$\eta_{conc} = OCV(SOC_{surface},T) - OCV(SOC_{average},T) \quad (5)$$

2.2 The energy conservation within the cell

The general equation for energy conservation is given in Eq. (6).

$$\rho c_p \left(\frac{\partial T}{\partial t} + v.\nabla T\right) = \nabla.k\nabla T + \dot{q} \quad (6)$$

The general energy conservation equation defines the temperature distribution within the cell. The heat dissipation rate to the surroundings can be evaluated from Eq. (7) where the first term on the right-hand side represents the convective heat dissipation and the second term shows the radiative heat dissipation rate.

$$n.(k\nabla T) = -h(T - T_{surr}) - \varepsilon\sigma(T^4 - T_{surr}^4) \quad (7)$$

The lumped battery model defines the heat transfer interface for three solids that constitute the cell such as a mandrel, active battery material, and the canister. The Eq. 6 and Eq. 7 are applied in each solid. The emissivity of the cell's surface was taken as 0.3. The Churchill-Chu correlation method is used to adjust the variable convective heat transfer coefficient (h) for natural convection condition.

2.3 Electrochemical heat source

The heat generation within the cell is derived from Bernardi et al. [3] is usually used as the simplified form as stated in Eq. (8).

$$\dot{Q} = I(OCV - V) - I\left(T\frac{\partial OCV}{\partial T}\right) \quad (8)$$

The first term on the right-hand side is specified the irreversible heat generation within the cell. The second term represents the reversible heat generation which includes the entropic heat coefficient, the derivative of the open circuit potential with respect to temperature. The lumped battery model predicts the heat generation of the cell using Eq. (9) [10].

$$Q_{gen} = I_{cell}\left(\eta_{ohmic} + \eta_{act} + T\frac{\partial OCV(SOC_{surface},T)}{\partial T}\right) + Q_{mix} \quad (9)$$

2.4 Experimental set up

The following components are used to investigate the thermal behavior of the Li-ion batteries.
i. Maccor 4300 Test Equipment.
ii. Nüve FN300 Oven.
iii. Cylindrical Li-ion batteries.
iv. T, K and J type thermocouples.
v. NI-DAQ (National Instrument Data Acquisition) device. Fig.2 shows the testing system which is used to examine the thermal behavior of Li-ion batteries by applying simulated loads under computer control.

Fig. 2. Battery testing system.

3 Results and discussion

3.1 Determination of the constant specific heat value of the cell

The constant specific heat (c_p) value of the cell was measured using the Lumped Transient Model (LTM). A cylindrical aluminium specimen and the Li-ion cell were heated up until they reach a certain surface temperature around 50°C. Then their cooling behaviour were observed as stated in Fig. 3. As a result, c_p value of the cell was determined as 0.75 kJ/kgK.

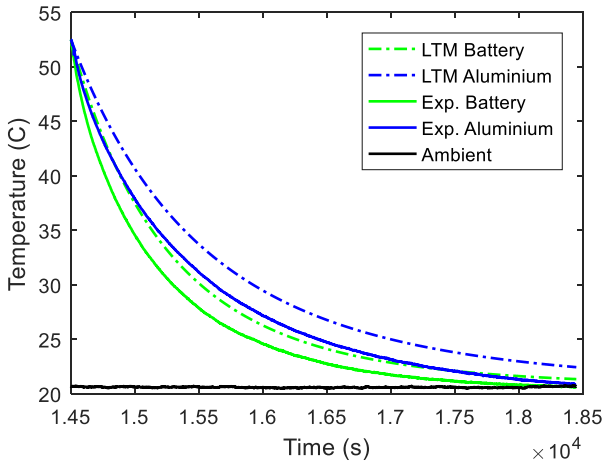

Fig. 3. Cooling behavior of the Aluminum specimen and the Li-ion battery cell.

3.2 The entropic term mapping

In this study, the variation of the entropic term as a function of SOC was neglected for each discharging process and operating temperature. The entropic term was assumed constant and determined so as to predict the experimental temperature variation of the cell over time. The mapping results were presented in Table 2.

Table 2. Entropic Term Mapping Results

Entropic Term (mV/K)	0°C	20°C	50°C
0.5C	0.58	0.34	0.3
1.0C	0.6	0.53	0.42
1.5C	0.8	0.66	0.6

3.3 Comparison of the model and experimental results during 0.5-1-1.5C discharging processes at 0-20-50°C ambient temperatures

A series of experiments were conducted in order to examine the electrical and thermal performance of the batteries. One of the adverse effects of discharging the cell at cold ambient is observing high internal resistance values as it is stated in Fig. 4. The internal resistance of the cell varies with the temperature, DOD and the discharge rate of the cell. It can be seen from Fig. 4 that the cell resistance increases as the temperature decreases.

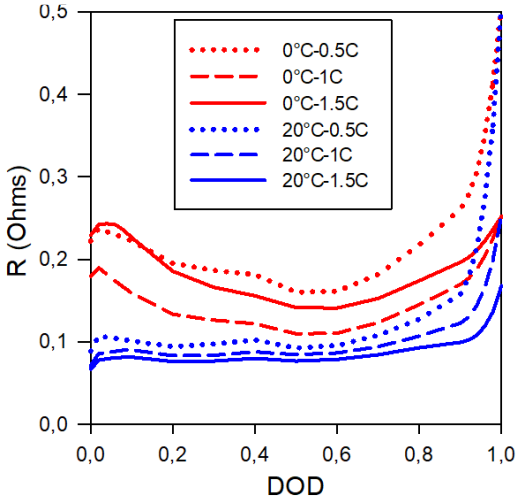

Fig. 4. Internal resistance of the cell during various discharging processes at 0°C and 20°C.

High resistance increases the heat generation within the cell so that the temperature of the cell increases as the discharging process continues, even though the more heat is dissipated by conduction and convection. The developed model is used in order to observe the thermal behavior of the cell. The model is valid in between 1-0.2 SOC values since the internal resistance of the cell can be assumed as constant in this interval. The temperature difference between the cell surface and the ambient is obtained from both experiments and the simulations. The results were presented in Fig. 5.

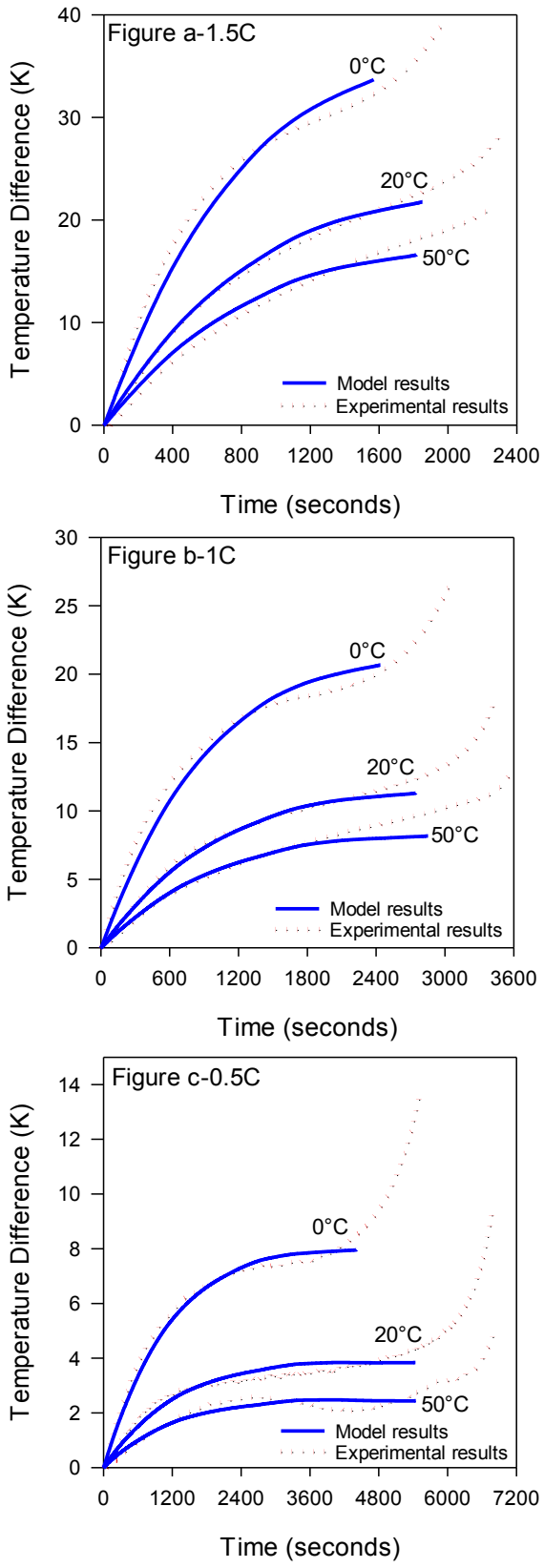

Fig. 5. Comparison of the temperature difference between the ambient and the surface of the cell during (a) 1.5C, (b) 1C, (c) 0.5C rate discharging processes at 0-20-50°C.

The simulation results at 0°C are slightly different from experimental results since the characteristics of the cell changes at low temperatures. Fig. 5 shows that the operating temperature has considerable effects on cells thermal behavior. The temperature of the cell increases as the operating temperature decreases. Besides, the cell temperature increase is more pronounced at high C-rates as expected.

The heat is dissipated from the cell by natural convection and radiation. Fig. 6 compares the dissipated radiative heat rates with the convective heat rates during various discharge rates at 50°C. The results show that the effect of radiation cannot be disregarded.

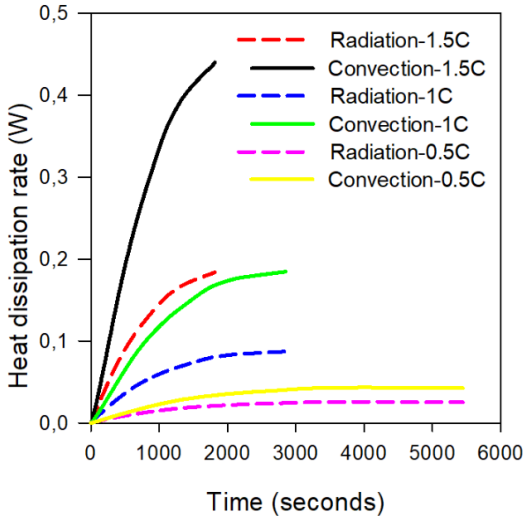

Fig. 6. Comparison of the dissipated heat rates by natural convection and radiation at 50°C.

Fig. 7 indicates the variation of the convective heat transfer coefficient during 0.5-1-1.5C discharging processes at 50°C. The results show that the convective heat transfer coefficient can be assumed as constant at low discharge rates.

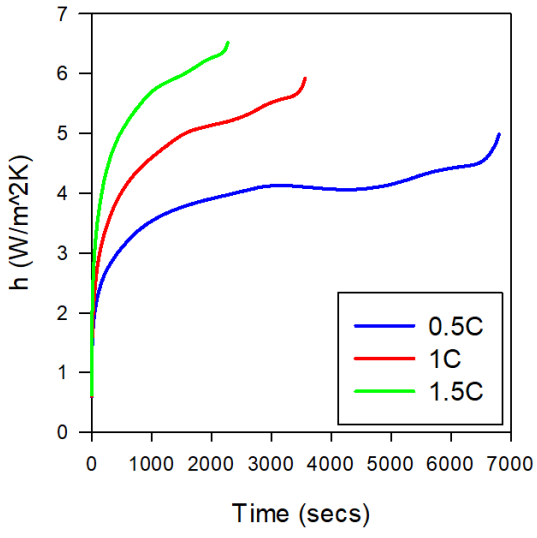

Fig. 7. Variation of the convective heat transfer coefficients during various discharging processes at 50°C operating temperature.

4 Conclusion

The thermal and electrical behavior of a cylindrical Li-ion battery cell is examined comparing the simulation

and the experimental results at various discharging processes and ambient temperatures. The results were found consistent.

The heat generation rate from the cell was obtained from Bernardi's equation calculating the reversible and irreversible terms. The heat diffusion equation was used to evaluate the temperature variation of the cell. The simulation results were more accurate at 20°C operating condition due to the stability of the cell resistance in a SOC range between 1-0.2. On the other hand, it was found that the temperature variation of the cell is greatly influenced by the operating temperature as it affects the heat generation within the cell.

The results show that the capacity of the cell significantly decreases at cold operating temperatures. Morever, the increment in cell resistance causes higher heat generation which also leads to a higher temperature increment within the cell during the discharging processes at cold ambients.

It can be concluded from the simulation results that the heat dissipation by radiation should not be neglected, especially at high discharge rates even though the natural convection affects the heat dissipation rate further.

References

1. Y. Nishi, J. Power Sources, **100,** 101 (2001)
2. J. Xie, Z. Ge, M. Zang, S. Wang, Appl. Therm. Eng., **126**, 583 (2017)
3. D. Bernardi, E. Pawlikowski, J. Newman, J. Electrochem. Soc., **132**, 5 (1985)
4. S. J. Bazinski, X. Wang, J. Electrochem. Soc., **161**, A168 (2013)
5. G. G. Botte, B. A. Johnson, R. E. White, J. Electrochem. Soc., **146**, 914 (1999)
6. K. Smith, C. Y. Wang, J. Power Sources, **160**, 662 (2006)
7. Y. Chen, J. W. Evans, J. Electrochem. Soc., **140**, 1833 (1993)
8. S. Al Hallaj, H. Maleki, J.S. Hong, J. R. Selman, J. Power Sources, **83**, 1 (1999)
9. V. Srinivasan, C. Y. Wang, J. Electrochem. Soc., **150**, A98 (2003)
10. Comsol Multiphysics Reference Manual, version 5.4", Comsol, Inc, www.comsol.com.